Title no. 107-S08

Pushover Analysis of Shear-Critical Frames: Verification and Application

by Serhan Guner and Frank J. Vecchio

An analytical procedure was recently developed for the nonlinear analysis of reinforced concrete frame structures consisting of beams, columns, and shear walls under monotonic and pushover loading. The advantage of the procedure lies in its inherent and accurate consideration of shear effects and significant second-order mechanisms within a simple modeling process suitable for use in practice. Herein, the application of the procedure to 33 previously tested specimens, two-thirds of which were shear-critical, is presented to verify the algorithms developed. Important considerations in nonlinear modeling are also discussed to provide guidelines for general modeling applications. The procedure is found to simulate the experimental behaviors of the specimens examined with a high level of accuracy. Experimental strengths, stiffnesses, ductilities, and failure modes were all calculated accurately. Computed parameters such as crack widths, reinforcement strains, and member deformations were also represented successfully. The procedure exhibits excellent convergence and numerical stability, requiring little computational time.

INTRODUCTION

In recent years, computer-aided nonlinear analysis procedures for reinforced concrete frame structures have progressed toward becoming a practical tool for use by office engineers. These procedures have found diverse applications, including the strength and safety assessment of existing structures and the performance assessment of planned structures. At the same time, research activity on the shear behavior of reinforced concrete continues to contribute to current knowledge. Design code procedures are continually evolving and generally becoming more stringent. This acknowledges the fact that shear-critical structures fail in a brittle and catastrophic manner with little or no prior sign of distress. Therefore, analysis methods that accurately consider shear effects are essential for the safe and realistic assessment of strength and ductility of concrete structures. Most currently available analysis tools, however, continue to ignore shear-related mechanisms by default. The use of such tools for practical applications, where the structure may be in fact shear-critical, can lead to dangerously unconservative estimates of both strength and ductility.

Consider, for example, the clinker plant preheater tower shown in Fig. 1. Designed according to ACI code specifications, the tower was built in a seismic zone of Central America in the late 1990s. Following its construction, subsequent design reviews revealed deficiencies in the amounts and details of the reinforcement provided in some of the beams and columns. These deficiencies raised questions about the expected performance of the building under its design earthquake, requiring a comprehensive reevaluation. More specifically, its load and displacement capacity, failure
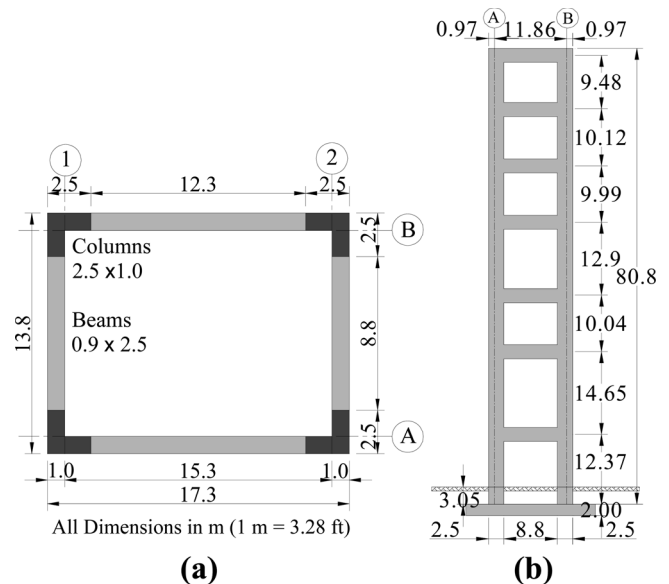

Fig. 1—Structural layout of clinker preheater tower: (a) plan; and (b) elevation.

mode, and any deficient members had to be verified. For analysis purposes, three software programs were used: SAP2000® (CSI 2005), RUAUMOKO (Carr 2005), and TEMPEST (Vecchio 1987; Vecchio and Collins 1988). The frame was modeled using only default options and models that were readily built into the programs, that is, default hinges and all default material behavior models. All three models were created using the same geometry, material, and support conditions. The analyses were performed under monotonically increasing static story shear forces calculated by the linear dynamic response spectrum method.

From these analyses, unacceptably different results were obtained, as shown in Fig. 2. SAP2000 and RUAUMOKO predicted that the frame would fail in flexure, while TEMPEST predicted a sudden shear failure in some of the beams. Large discrepancies were obtained in the ductility predictions for the frame; SAP2000 predicted approximately 5.6 times greater displacement for the peak load capacity than did TEMPEST. The highly ductile load-deflection prediction obtained from SAP2000 and RUAUMOKO resulted from the assumption of purely flexural behavior. In other words, the influence of the shear-related mechanisms

ACI member **Serhan Guner** is a Structural Designer at Morrison Hershfield Limited, Toronto, ON, Canada. He received his PhD in 2008 from the University of Toronto, Toronto, ON, Canada. His research interests include nonlinear analysis and performance assessment of reinforced concrete structures, shear effects in reinforced concrete, and structural dynamics and seismic response.

Frank J. Vecchio, FACI, is a Professor of civil engineering at the University of Toronto. He is a member of Joint ACI-ASCE Committees 441, Reinforced Concrete Columns, and 447, Finite Element Analysis of Concrete Structures. He received the 1998 ACI Structural Research Award and the 1999 ACI Structural Engineering Award. His research interests include advanced constitutive modeling and analysis of reinforced concrete, assessment and rehabilitation of structures, and response under extreme load conditions.

Fig. 2—Load-deflection response predictions for clinker preheater tower.

was completely neglected in the default moment hinges used. In the TEMPEST analysis, on the other hand, the default material behavior models considered inelastic shear effects and predicted shear failures for the upper-story beams, thereby providing the least ductile response. Note that, with the TEMPEST analysis, deteriorating convergence factors and large unbalanced shear forces became apparent beyond a base shear force of 6300 kN (1418 kips), raising questions about the validity of the load-deflection curve afterwards. If one were able to anticipate a shear-dominated behavior prior to the analyses, it would have been possible to create user-defined custom shear hinges in SAP2000 and RUAUMOKO models. Such analyses, however, would have required expert knowledge on the shear-behavior of reinforced concrete in addition to specialized supporting software to develop the shear-hinge models and would have taken significant engineering time and effort.

An analysis procedure was recently proposed by Guner and Vecchio (2010) to inherently and accurately account for shear-related effects coupled with axial and flexural mechanisms in nonlinear frame behavior. The iterative procedure uses nonlinear sectional analyses in a stiffness-based linear-elastic frame analysis algorithm through the use of an unbalanced force approach. A layered (fiber) representation is used in the nonlinear sectional analyses, in which the cross section is discretized into a number of concrete, reinforcing, and prestressing steel layers. Each layer is then analyzed for two-dimensional in-plane strain conditions according to the equilibrium, compatibility, and constitutive requirements of the disturbed stress field model (DSFM) (Vecchio 2000). The equilibrium requirements include balancing the axial force, shear force, and bending moment calculated by the frame analysis, whereas the main compatibility requirement is that "plane sections remain plane." The clamping stresses in the transverse direction are assumed to be zero. A shear-strain-based analysis with parabolic distribution is used, which permits the analysis to continue in the post-peak region. The procedure allows the analysis of frames with unusual or complex cross sections under a large range of static and thermal load conditions. In addition to its rigorous consideration of shear effects, the procedure has advantages over others with its simple modeling requirements suitable for use by practicing structural engineers. The procedure does not require a user to select appropriate analysis options and parameter values, does not require pre-analysis supporting calculations such as shear force-shear deflection responses or hinge definitions, does not require the analyst to anticipate the behavior and failure mechanism prior to the analysis, and is fast and numerically stable.

This paper discusses the application of the proposed procedure to 33 previously tested structures consisting of beams, frames,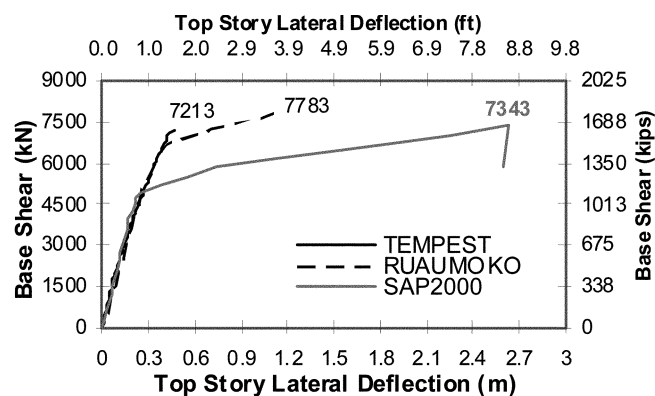 and shear walls to verify the newly implemented algorithms. As the main focus is to accurately simulate shear-related mechanisms, two-thirds of the specimens selected exhibited shear-dominated behavior in the experiments. Important considerations in nonlinear modeling are also discussed through the use of practical examples, with the aim of providing guidelines for general modeling applications.

RESEARCH SIGNIFICANCE

Unlike flexure-critical structures that typically exhibit ductile failure modes, shear-critical structures fail in a much less forgiving brittle manner with little or no forewarning. When shear-related mechanisms are neglected in analytical assessments of such structures, grossly unconservative calculations of strength and ductility predictions can result. Most available tools, however, ignore shear effects by default; those that do consider them are often difficult to use and still inaccurate. Thus, improved procedures are needed because shear-critical structures continue to be found in practice. To address this deficiency, an analysis procedure was recently proposed by Guner and Vecchio (2010). This paper describes verification studies examining the accuracy of the proposed formulations and provides guidelines for general modeling applications.

MODELING OF SHEAR-CRITICAL BEAMS

The first group of specimens examined was that tested by Vecchio and Shim (2004), involving four sets of three beam series subjected to monotonically increasing point loads. The beams were designed to be shear-critical, with shear reinforcement ratios ranging from 0.0 to 0.2%. Displacement-controlled loading was applied at the midspans, producing shear span-depth ratios ranging from 3.3 to 5.8. The beam cross sections had a depth of 552 mm (21.7 in.) and widths of 305, 229, and 152 mm (12, 9, and 6 in.) for beam Series A, B, and C, respectively. The longitudinal reinforcement ratios used ranged from 1.4 to 3.2%; the concrete compressive strengths ranged from 22.6 to 43.5 MPa (3.3 to 6.3 ksi).

In the creation of a frame model, the frame elements should be divided into reasonably short members (that is, segments) to ensure that the average member forces are calculated with sufficient accuracy for use in the nonlinear analyses. For optimal accuracy, the recommended member length is in the range of 50% of the cross section depth for beam and column members and 10% of the cross section depth for shear wall members. Frame models of the beams
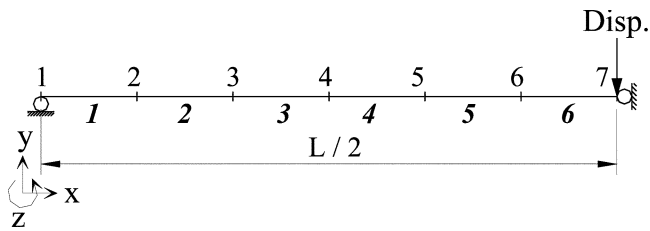
Fig. 3—Frame model for Vecchio and Shim (2004) and Angelakos et al. (2001) beams.
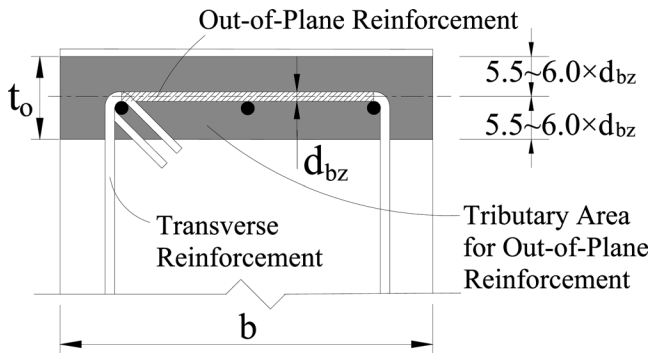

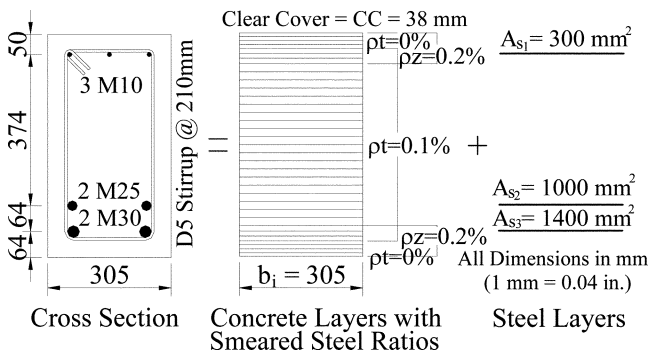*Fig. 4—Determination of tributary area for out-of-plane reinforcement.*

Fig. 5—Sectional model for Beam VS-A1.

Table 1—Concrete layers and assigned reinforcement ratios for Beam VS-A1

D_c, mm (in.)	ρ_t, %	ρ_z, %	N
8 (0.3)	0	0.20	1
10 (0.4)	0	0.20	3
12 (0.5)	0.10	0.20	2
14 (0.6)	0.10	0.20	1
20 (0.8)	0.10	0	20
14 (0.6)	0.10	0.20	1
12 (0.5)	0.10	0.20	2
10 (0.4)	0	0.20	3
8 (0.3)	0	0.20	1

Consideration of out-of-plane reinforcement is particularly important for layers under compression. A tributary area enclosed by approximately 5.5 to 6.0 times the bar diameter is suggested for the calculation of the out-of-plane reinforcement ratio as follows

$$\rho_z = \frac{A_b}{s_t \times t_o} \quad (1)$$

where A_b is the cross-sectional area of the out-of-plane reinforcement, s_t is the spacing of the out-of-plane reinforcement in the longitudinal (x) direction, and t_o is the distance, in the transverse (y) direction, in which the out-of-plane reinforcement is to be assigned.

The transverse reinforcement is assigned to the concrete layers between the out-of-plane reinforcement, with the ratio defined as follows

$$\rho_t = \frac{n \times A_b}{s_t \times b} \quad (2)$$

where n is the total number of legs extending in the transverse direction and b is the width of the concrete layer in which the assignment is to be made. The resulting reinforcement ratios are listed in Table 1, where D_c is the concrete layer thickness and N is the total number of concrete layers with the same thickness and reinforcement ratios. For Beam VS-A1, the sectional model used is shown in Fig. 5. More detailed information regarding the modeling and analysis process can be found in Guner (2008) and Guner and Vecchio (2008).

The analytically and experimentally obtained midspan load-deflection responses for the Vecchio and Shim (2004) beams are compared in Fig. 6. The peak load capacities of the beams were calculated with good accuracy; the ratio of the calculated-to-observed ultimate load for all 12 beams had a mean of 1.05 with a coefficient of variation (COV) of 6.1%. The midspan deflections at maximum loads were calculated with a reasonable calculated-to-observed mean ratio of 0.82 and a COV of 12.8%. The general tendency in the analytical results was to underestimate deflections, giving stiffer responses than the experimental responses. Analyses of these beams with a more rigorous finite element tool also provided similarly stiffer responses (Vecchio and Shim 2004). The softer experimental behaviors may possibly be attributable to the irregularities in the test setup.

Failure displacements are particularly important when determining the ductility of structures. For these beams, they were calculated with a mean of 0.93 and a COV of 18.3%.

were created for only one-half of each beam, taking advantage of symmetry, as shown in Fig. 3. The vertical degree-of-freedom at Node 1 was restrained to define a simple roller; both the horizontal and rotational degrees of freedom at Node 7 were restrained to satisfy the condition of symmetry.

For the creation of sectional models, a discretization of 30 to 40 concrete layers typically provides satisfactory results. Because the longitudinal strain distribution reaches maximum values at the top and bottom of the cross sections, concrete layer thicknesses preferably should be reduced in these regions, especially on the compression side of the section. For general applications, a symmetrical layout for the concrete layer thicknesses is recommended, as was used throughout this study.

Determination of the concrete layer thicknesses requires particular attention to the clear cover thickness and the out-of-plane reinforcement configuration. As an example application, consider Beam VS-A1, which had a clear cover of 38 mm (1.5 in.) and a closed stirrup fabricated from a 6.4 mm (0.25 in.) diameter bar. The legs of the stirrups extending in the out-of-plane direction constitute the out-of-plane reinforcement, as shown in Fig. 4.
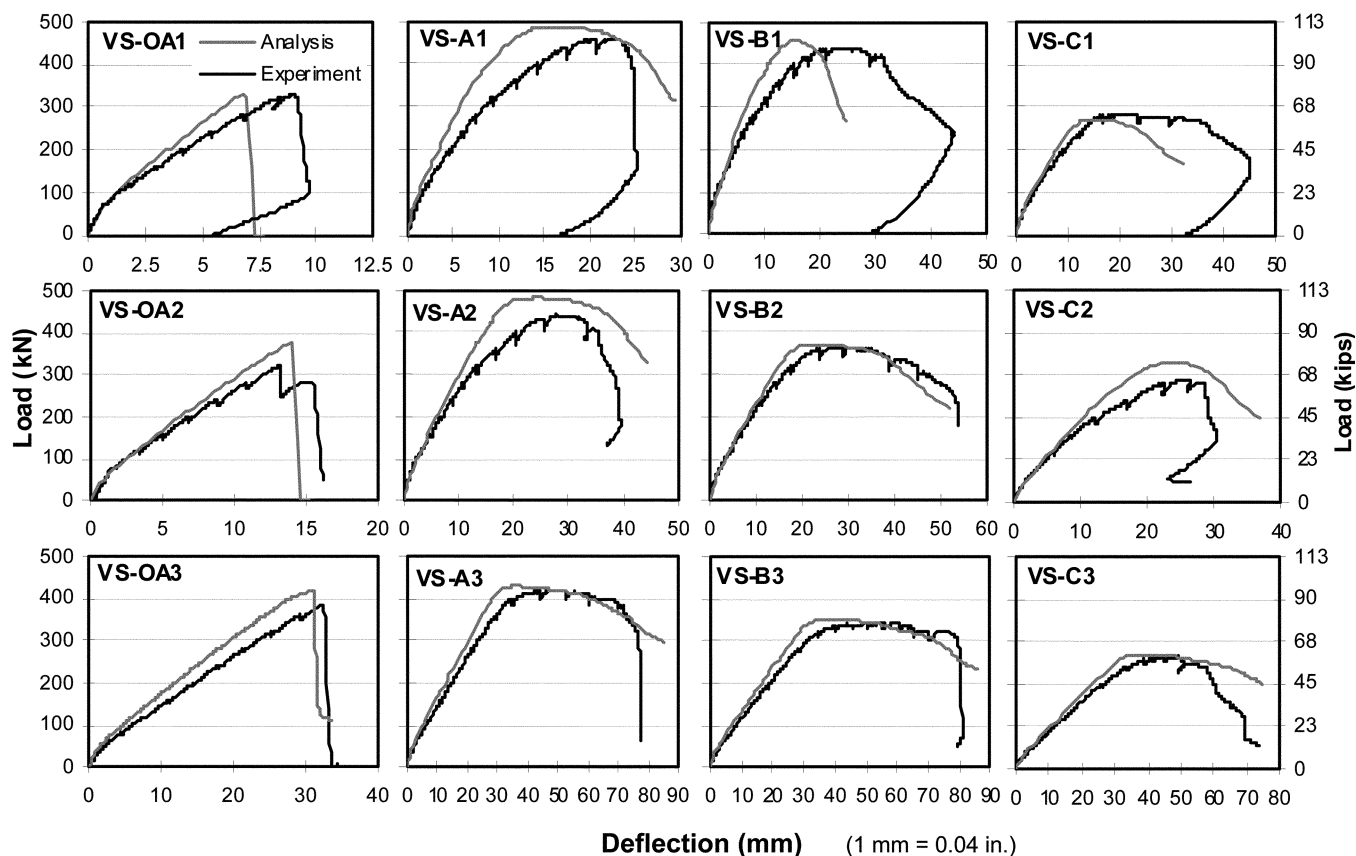
Fig. 6—Comparison of midspan load-deflection responses for Vecchio and Shim (2004) beams.

The more scattered nature of these results should be expected since the post-peak ductility of shear-critical beams containing little or no shear reinforcement is largely governed by mechanisms heavily dependent on the concrete tensile strength, itself a property prone to wide scatter. Three different failure modes were reported in the experimental study: diagonal tension failures for all three beams containing no shear reinforcement; shear-compression failures for the intermediate-span beams containing shear reinforcement; and flexure-compression failures for the long-span beams containing shear reinforcement. For all twelve beams, these failure modes were calculated accurately by the analyses.

A second series of beams examined was that tested by Angelakos et al. (2001), involving 12 beams subjected to monotonically increasing point loads applied at their midspans in a displacement-controlled mode. These beams differed from the Vecchio and Shim (2004) beams in three important aspects: the beam cross sections were larger with 1000 x 300 mm (39.4 x 11.8 in.) dimensions; the shear span-depth ratios were lower at 2.7; and the longitudinal reinforcement amounts were smaller with uneven distributions. With large cross sections and low transverse reinforcement ratios ranging from 0.0 to 0.08%, size effects, aggregate interlock, concrete post-cracking tensile stresses, and crack slip are expected to be significant mechanisms in the behavior of these beams. Furthermore, with the lower shear span-to-depth ratio, concrete direct strut action, which is neglected in the sectional calculations of the proposed procedure, will play a more significant role in the responses. Some of these beams were fabricated with high-strength concrete, representing an additional challenge.

The strength of beams containing little or no reinforcement is highly sensitive to such mechanisms as tension softening, tension stiffening, and aggregate interlock, all of which are directly related to the tensile strength of concrete. The tensile strength of concrete, however, is not constant relative to the compressive strength but varies with a number of parameters such as the volume of concrete, gradient of longitudinal strain, and the presence of restrained shrinkage strains (Collins and Mitchell 1991). A lower-bound estimate of the tensile strength, given by Eq. (3) as recommended by CSA A23.3-04, was used for all analyses in this paper. Consequently, when analyzing a specimen with no or little reinforcement, more scattered predictions should typically be anticipated.

$$f'_t = 0.33 \times \sqrt{f'_c} \qquad (3)$$

The frame models for these beams consisted of six members, taking advantage of symmetry to represent one-half of the beam length, as shown in Fig. 3. Sectional models were created using approximately 40 concrete layers in the same manner as the Vecchio and Shim (2004) beams. As recommended by Angelakos et al. (2001), the maximum aggregate size used in the analyses was taken as zero for the beams having concrete strengths greater than 65 MPa (9.4 ksi) (that is, for Beams DB165, DB165M, DB180, and DB180M) as cracks pass through, rather than going around the aggregate, causing aggregate interlock to be ineffective.

As shown in Fig. 7, the peak load capacities of the beams were calculated reasonably well with a mean of 1.07 and a COV of 16.7% for the calculated-to-observed strength ratio. The COV is somewhat higher than normally expected with
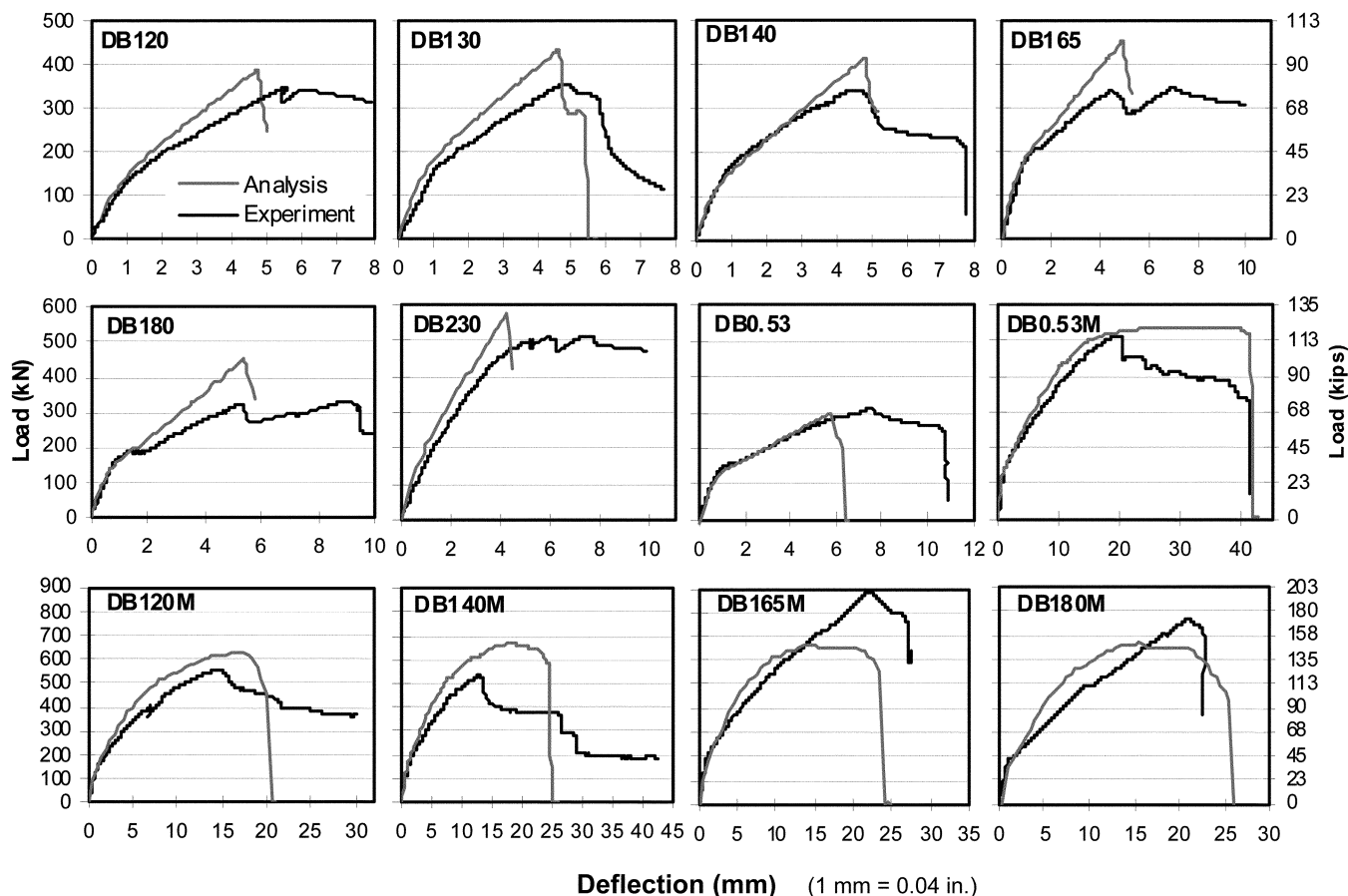
Fig. 7—Comparison of midspan load-deflection responses for Angelakos et al. (2001) beams.

nonlinear analyses for the reasons noted previously. The failure modes of all the beams were accurately calculated as diagonal-tension failures. For the specimens containing no shear reinforcement, the analytically determined failures occurred suddenly in the compression zone of Member 5, similar in nature to the experimental behavior. For the beams containing shear reinforcement, the calculated responses typically involved the failure of Member 2 with significantly more diagonal cracking prior to the failures, as compared to the beams containing no shear reinforcement. A diagonal-tension failure mode was also observed in the experiments with diagonal cracks extending between the point load at the midspan and the support.

MODELING OF FRAMES

The first frame specimen examined was that tested by Duong et al. (2007), involving the one-bay, two-story frame shown in Fig. 8(a). The test frame was designed to imitate the details of the clinker preheater tower described previously, reproducing the shear deficient characteristics of the beams: the beams' span-depth ratio, shear and longitudinal reinforcement amounts, and material strengths. The testing of the frame was performed in two phases: Phase A for a single cycle, consisting of a forward and reverse loading, and Phase B, for a sequence of complete cycles after the frame had been repaired with fiber-reinforced polymer (FRP) wrap. In both phases, a monotonic lateral load was applied to the second-story beam in a displacement-controlled mode, while two constant column loads were applied throughout the testing to simulate the axial force effects of higher stories.

A frame model of the structure was created using member lengths approximately equal to half of the cross section depth, that is, 200 mm (7.9 in.). Because frame models are typically based on centerline dimensions, stiffened end zones are normally used to account for the overlapping portions of the beams and columns in the joint regions, as shown with bold lines in Fig. 8(b). One way of achieving this is to increase both the longitudinal and transverse reinforcement amounts in the end zone members. Based on a limited study, a multiplier of 1.5 or larger was found to perform satisfactorily for this purpose; a factor of 2 was used throughout this study. The bolts used in the experiment to fix the base beam to the strong floor were represented by simple supports. Six member types were used to create the sectional models of the beam, column, and base members. An additional six member types were used for the stiffened end zone members. Typically, 30 concrete layers were used, as shown in Fig. 8(c). Refer to Guner (2008) for the complete details of the sectional models.

In the experimental study, once significant shear damage took place, the frame was unloaded to prevent total failure; the frame was to be retrofitted and retested in the Phase B program. Because a determination of the failure condition was desired in this analytical assessment, however, the frame was loaded to failure. As shown in Fig. 9, the frame's maximum load capacity was calculated with good accuracy, having a calculated-to-observed ratio of 1.06. The gradual decrease in the lateral stiffness in the prepeak region was captured well. In addition, the lateral load levels causing the first yielding of several reinforcement components were
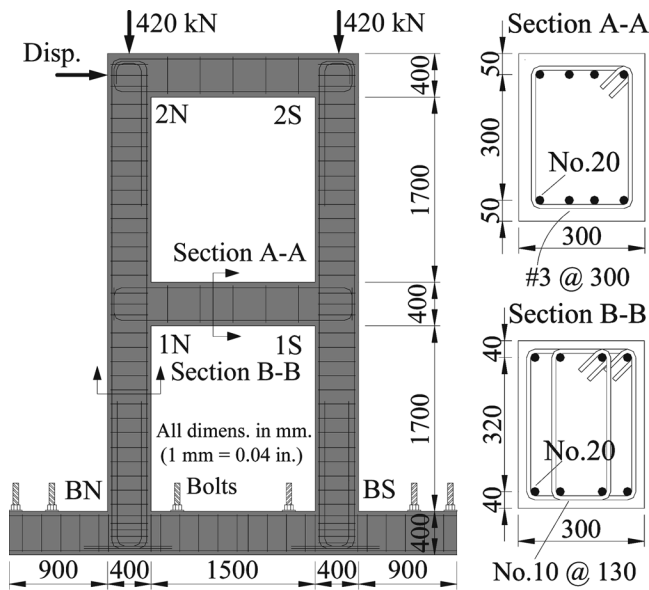
(a)
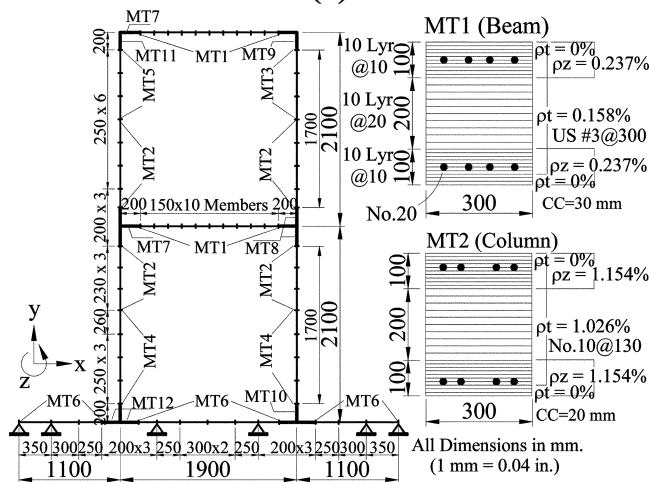
(b)   **(c)**

Fig. 8—Duong et al. (2007) frame: (a) structural details; (b) frame model; and (c) sectional models.

Fig. 9—Comparison of load-deflection responses for Duong et al. (2007) frame.

Fig. 10—Structural details of Vecchio and Emara (1992) frame.

Fig. 11—Comparison of load-deflection responses for Vecchio and Emara (1992) frame.

estimated reasonably. The calculated crack widths also showed a strong correlation to the experimental crack widths, as documented in Guner (2008). The damage mode of the frame was experimentally classified as flexure-shear with significant shear damage of Beam 1N accompanied by flexural mechanisms involving flexural cracking and reinforcement yielding. A similar failure mechanism was determined analytically. The first drop in the load capacity of the frame, at 48 mm (1.9 in.) displacement, was caused by the shear failure of Beam 1S. Because the top-story beam was intact, the frame continued to carry increased deformations until a shear failure of Beam 2S, at 68 mm (2.7 in.) displacement, which caused the second drop in Fig. 9. After that, the only remaining load-resisting mechanism was a cantilever column.

The second frame specimen investigated was that tested by Vecchio and Emara (1992). This frame differs from the Duong et al. (2007) frame in three important aspects: the frame was flexure-critical with well-confined cross sections; the beams' span-depth ratios were larger at 8.75; and, lastly, higher column axial loads were applied, as shown in Fig. 10.
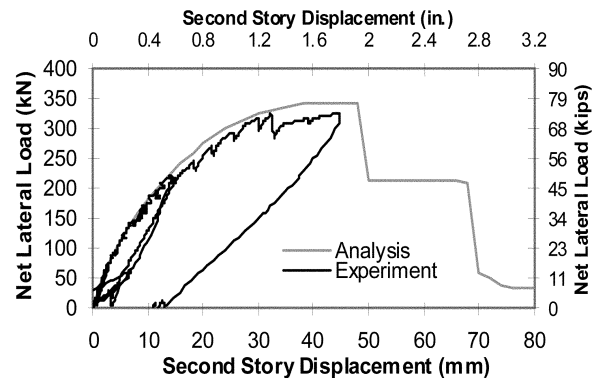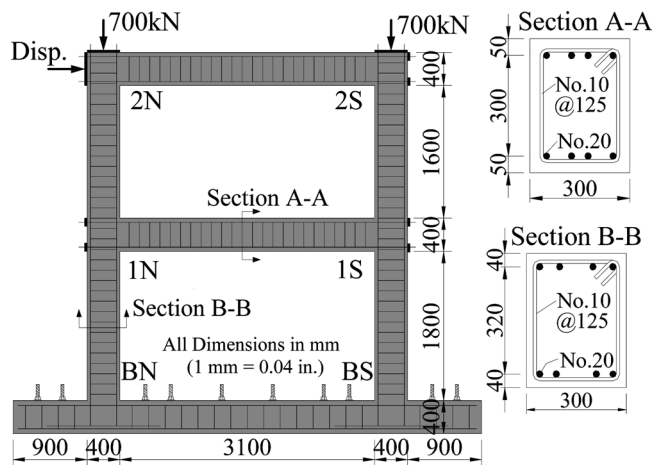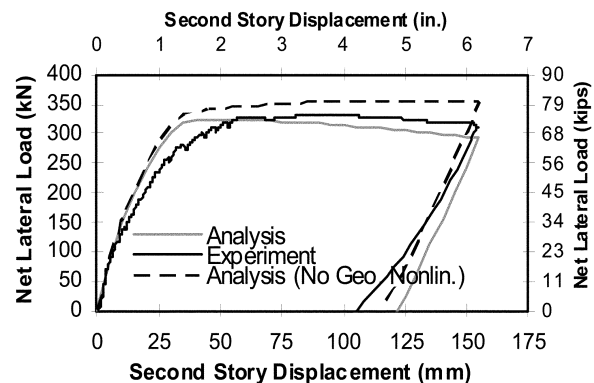
The frame model for this specimen was created using member lengths in the range of half of the cross section depth; that is, 200 mm (7.9 in.). Stiffened end zones were used for the reasons explained previously. Three member types were used to create sectional models of the beam, column, and base members; three additional member types were used for the stiffened end zones of these members. Typically, 40 concrete layers were used in the sectional models (refer to Guner [2008] for the details of the frame and sectional models). The frame was loaded to a lateral displacement of 155 mm (6.1 in.) and then unloaded to a net lateral load of zero, as was done in the experiment.
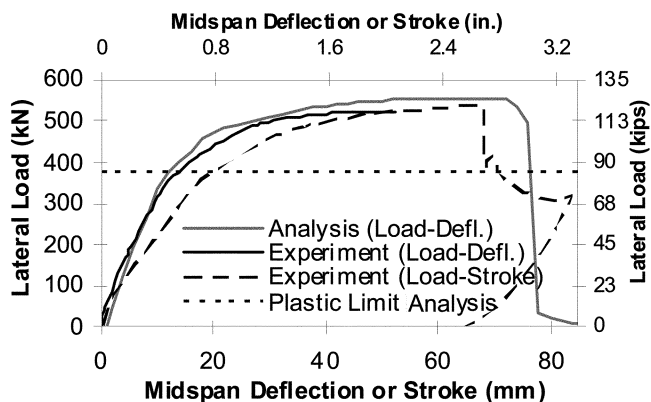
Fig. 12—Comparison of responses for Vecchio and Balopoulou (1990) frame.

As apparent from Fig. 11, the frame's maximum load capacity was estimated with excellent accuracy, having a calculated-to-observed ratio of 0.98. The lateral stiffness of the frame was calculated with reasonable accuracy. Upon entirely unloading the frame, the residual displacement was calculated with 14% overestimation. The total energy dissipated by the frame was calculated with high accuracy: 44.6 kNm (32.9 kips-ft) compared to the experimental value of 44.4 kNm (32.7 kips-ft). The experimentally observed damage mode of the frame involved ductile plastic hinging of both beam ends (Beam 1N, 1S, 2N, and 2S) and both column bases (BN and BS), including yielding of both the tension and compression reinforcement and some concrete crushing. The analytical damage mode was mainly caused by the plastic hinging of the column bases, including yielding of both tension and compression reinforcement and crushing of concrete, especially in the BS area. The first- and second-story beams ends were calculated to be extensively damaged with crack widths as high as 9.0 mm (0.35 in.) and tensile reinforcement strains reaching 47×10^{-3}. The compression reinforcement at the beam ends, however, did not yield but typically reached 80% of their yield strain in the analysis (Guner 2008).

Of particular interest in the behavior of this frame is the influence of the second-order effects (that is, P-Δ effects), which accounted for 12% of the total overturning moment acting on this frame at ultimate. For illustrative purposes, the analysis was repeated without considering geometric nonlinearity based on a small displacements assumption. As shown in Fig. 11, the net lateral load continued increasing with the increased lateral displacement, causing an overestimation of the frame's strength. Of another interest is the effect of shear deformations on the response of this frame. As a result of an investigation, the Vecchio and Emara (1992) concluded that shear deformations contributed to the total deformations of this frame as much as 20%, despite a predominantly flexural failure mode.

The third frame investigated was that tested by Vecchio and Balopoulou (1990). This frame was almost identical to the Vecchio and Emara (1992) frame shown in Fig. 10. The only significant difference, other than the loading condition, was that the top reinforcement was cut back to two No. 20 bars in the central 500 mm (19.7 in.) length of the first-story beam. The loading of this frame involved applying a monotonically increasing vertical load in the center of the first-story beam until the failure occurred.

Taking advantage of the symmetry of the test setup, only one-half of the frame was modeled with member lengths in the range of half of the cross section depth, that is, 200 mm (7.9 in.). Four member types were used to create sectional models of the beam, column, and base members. Three additional member types were used in the stiffened end zones of these members. Concrete shrinkage strains of -0.5×10^{-3} were also applied to all members in the model, reflecting the degree of shrinkage reported by Vecchio and Balopoulou (1990).

The analytically and experimentally obtained first-story midspan load-deflection responses are compared in Fig. 12. The experimental load-deflection response reported by Vecchio and Balopoulou (1990) was terminated well before the failure of the frame for equipment safety reasons; hence, the stroke-deflection response for the complete test, as measured by the loading machine including the flexibility of the machine, is also compared to the analytical load-deflection response in Fig. 12. The analytical load-deflection response showed excellent agreement with the experimental response. The frame's strength, stiffness, and failure deflection, the latter being particularly important when calculating the frame's ductility, were calculated accurately. The maximum flexural crack widths were also calculated with reasonable accuracy, as shown in Table 2. The experimental failure mode of the frame involved a combination of a flexural collapse mechanism (that is, a three-hinge mechanism formed at the ends and the midspan of the first-story beam) and a final shear failure near the midspan of the first-story beam. A similar failure mechanism was calculated analytically with the plastic hinges forming under approximately 20% larger applied loads.

Of particular interest in the behavior of this frame are the axial restraint effects caused by the columns, commonly known as "membrane action." Subjected to monotonic loads, the first-story beam of the frame elongated due to the average tensile strains on the tension face being much larger in magnitude than the compressive strains on the opposing face. The columns, however, provided axial restraint and thus induced axial compression forces in the beam. The accurate calculation of this second-order axial force is essential for the accurate simulation of the frame behavior because the axial force can significantly increase the shear and flexural strength of the beam. To show the significance of this effect, a first-order plastic analysis of the frame was performed with a simple three-hinge mechanism assumed for the first-story beam. For the applied midspan load P_u of 380 kN (85.4 kips) and using a linear-elastic frame analysis, the axial force in the beam was determined as -12 kN (-2.7 kips), the shear force as 190 kN (42.7 kips), and the moment at the midspan as 190 kNm (140.1 kips-ft). A nonlinear sectional analysis was then performed, finding the shear and moment
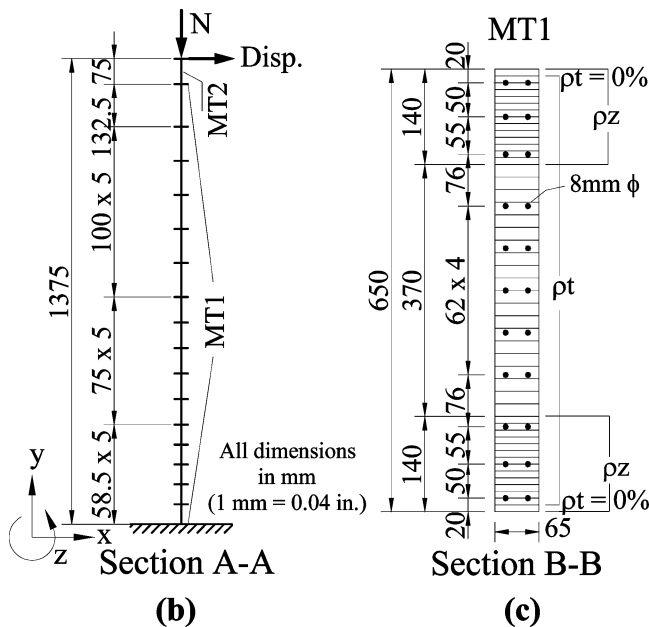
(a)

(b)   **(c)**
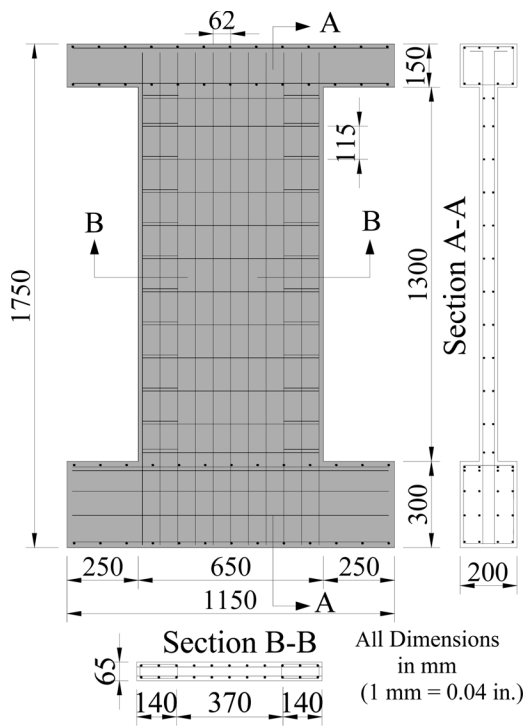
Fig. 13—Lefas et al. (1990) shear walls: (a) structural details; (b) frame model; and (c) sectional model.

capacities as 220 kN (49.5 kN) and 186 kNm (137.2 kips-ft), respectively. Hence, a flexural failure was predicted at P_u = 380 kN (85.4 kips), 30% less than the actual failure load. This underestimation occurred because the linear-elastic frame analysis calculated the axial compression force in the beam to be much less than the experimental value. In addition, the failure mechanism was determined incorrectly to be a flexural failure of the midspan section; in fact, a shear failure was observed near the midspan. This shows the necessity of nonlinear frame analysis procedures incorporating second-order effects, such as membrane action, for accurate simulations of the frame behavior.
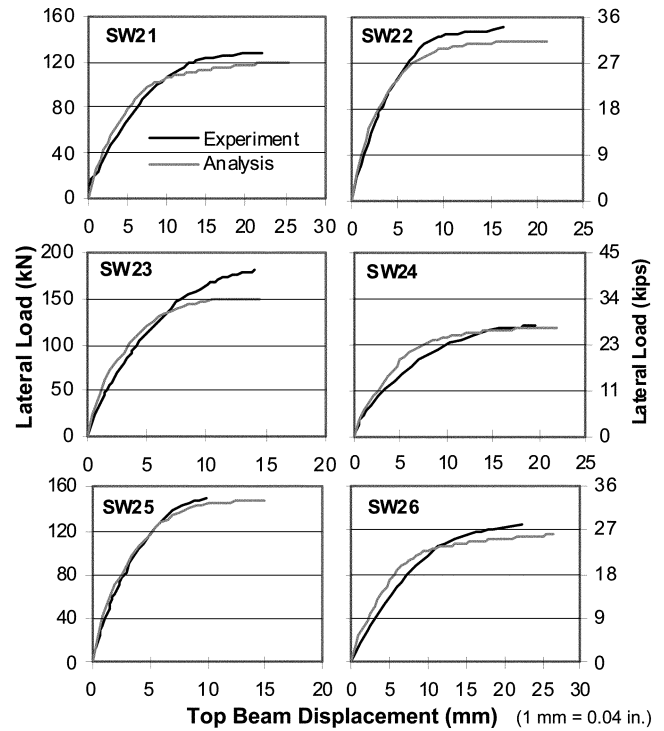

Fig. 14—Comparison of load-deflection responses for Lefas et al. (1990) shear walls.

MODELING OF SHEAR WALLS

The shear wall specimens examined here were the Type II walls tested by Lefas et al. (1990), having shear span-depth ratios of 2.1, as shown in Fig. 13(a). The walls were subjected to monotonically increasing horizontal loads, applied on the top spreader beams. Constant axial loads were applied on some of the walls as well. Note that shear walls with shear span-depth ratios of less than 2.0 are prone to significant direct strut action and thus are not appropriate for modeling with procedures based on layered sectional analysis.

The frame models of the walls were created with varying member lengths. A length of 58.5 mm (2.3 in.) (approximately 10% of the wall width) was used toward the base of the walls, where a concentration of plastic deformation was expected. The member lengths were gradually increased toward the top, as shown in Fig. 13(b). The base beam was not modeled; rather, the walls were assumed to be fixed at the base. One member type, discretized into 48 concrete layers (10.0 mm [0.4 in.] x 14 layers, 18.5 mm [0.7 in.] x 20 layers, and 10.0 mm [0.4 in.] x 14 layers) as shown in Fig. 13(c), was used for the sectional model. To simulate the top loading beam, an artificial member type was created by multiplying the reinforcement ratios of the first type by a factor of 2. Local conditions at the region through which the load is introduced are not particularly important in the sectional calculations. Out-of-plane reinforcement was assigned to the layers constituting the concealed columns at the flange edges, and transverse reinforcement was assigned to all layers except the 10 mm (0.4 in.) thick clear-cover layers.

As shown in Fig. 14, the strengths of the walls were calculated reasonably well with a mean of 0.93 and a COV of 5.5% for the calculated-to-observed strength ratio. The slight underestimation of the strengths is likely associated with some measure of direct strut action having occurred in the walls, given their shear span-depth ratios of 2.1. The lateral stiffnesses of the walls were also calculated reasonably well. The

general tendency was to slightly underestimate the experimental deflections, thereby giving slightly stiffer responses. Note that, in the experiments, reinforcement strain penetration into the wall bases may have noticeably affected the lateral stiffnesses of the walls. In the analyses, however, the base beams were not included in the model; a fixed base assumption was made. Note that for the walls with constant axial forces (that is, SW22, SW23, and SW25), the analytical underestimations of the deflections are minimal. This can be attributed to less strain penetration into the bases in these experiments.

The lateral loads causing the first yielding of the longitudinal reinforcement were calculated with a reasonable calculated-to-observed mean of 0.92 and a COV of 7.7%. The discrepancy to the low side may be associated with the softening effect of the base beam in the experiment. The experimental behaviors of the walls typically involved flexural mechanisms with the final failures caused by crushing of the concrete in the compression toe, which was initiated by near vertical cracks reaching the toe. Similar flexure-dominated behaviors were obtained for all of the walls in the analytical study.

CURRENT LIMITATIONS AND RECOMMENDATIONS FOR FUTURE WORK

As is typical with frame analysis of this type, the procedure uses centerline dimensions of the cross sections together with stiffened joint panel zone members; therefore, failure modes involving beam-column joint panel zones cannot be captured. Such failures are typical for joints having improper reinforcement detailing or insufficient confinement. A nonlinear member type for beam-column joints is required to further improve the capabilities of the proposed procedure; future work will be directed in this area. For the present, however, in the case of unusual or improper joint panel zone reinforcement detailing, or in cases where analysis results indicate possible joint distress, a detailed nonlinear finite element analysis of the joint should be undertaken. The sectional forces determined by the proposed procedure can be an important asset for such analyses, providing more realistic estimates of the boundary zone forces than would otherwise be obtained from linear elastic analyses. A detailed discussion of the application of finite element procedures for frame joints can be found in Sagbas (2007).

The procedure assumes perfect bond between concrete and reinforcement; therefore, bond slip of reinforcing bars are neglected. In addition, longitudinal reinforcement buckling provisions are not currently incorporated into the procedure proposed. Future work will be directed toward including these important mechanisms.

DISCUSSION OF RESULTS

Considering all 33 structures modeled, two-thirds of which were shear-critical, a mean of 1.03 and a COV of 11.9% were achieved for the calculated-to-observed strength ratio. As for the failure displacements, a mean of 0.85 with a COV of 20.7% were obtained. Considering the challenges involved in modeling shear-critical structures, these ratios can be regarded as satisfactory, particularly because several of the structures considered were influenced by complex second-order mechanisms. The failure modes and total energy dissipations of the structures modeled were calculated accurately. In addition, computed parameters such as reinforcement strain responses, crack widths, and member deformations showed strong correlations with the experimental results. The stiffnesses of the structures examined were captured reasonably well with slightly stiffer analytical responses than the experimental responses.

The cement clinker preheater tower discussed at the outset was reanalyzed with the proposed procedure (VecTor5) to gauge the improvements made over the predecessor procedure (TEMPEST). As before, the calculated frame response was governed by shear failures of some of the upper-story beams at approximately the same level of top-story lateral displacement (0.47 m [1.5 ft]). The calculated lateral shear strength (5693 kN [1280 kips]), however, was 27% less than that found from TEMPEST; recall that the TEMPEST calculations exhibited some numerical instability and lack of convergence in the final load stages, causing it to somewhat overshoot the failure load. Throughout the VecTor5 analysis, excellent convergence factors and negligible unbalanced forces were realized, providing confidence in the validity of the load-deflection response computed. More details of this comparison are provided by Guner (2008).

It is notable that all analyses reported herein were performed with the use of default material behavior models and analysis options. No decisions regarding the expected behavior, failure mode, or selection of appropriate parameter values were made prior to the analyses. No additional calculations, such as moment-axial force or shear force-shear deformation responses of the cross sections, were performed. In addition, the analyses required little computation time. For the beams analyzed, approximately 1 minute was required; the longest analysis time of approximately 6 minutes, using a laptop computer, was required for the Duong et al. (2007) frame.

The newly implemented shear protection algorithm, which approximately takes into account the increased strengths of D-regions, performed well. Premature shear failures of sections adjacent to beam-column panel zones, point load application areas, and supports were prevented. The newly implemented shear failure check algorithm also performed well. Sudden shear failures of several structures (for example, DB0.53M, DB140M, and Duong et al. (2007) frame) were detected that would otherwise have gone unnoticed with significant unbalanced shear forces and gradually diminishing load-deflection responses.

SUMMARY AND CONCLUSIONS

An analytical procedure was developed for the nonlinear analysis of reinforced concrete frame structures under pushover and monotonic loads. The procedure employs nonlinear sectional analyses within a stiffness-based linear-elastic frame analysis algorithm through the use of an unbalanced force approach. The nonlinear sectional analyses are made to capture shear mechanisms through modeling based on the DSFM. Verification of the accuracy of the procedure was undertaken by performing analyses for 33 mostly shear-critical previously tested specimens. The results of the investigations conducted support the following conclusions:

1. Consideration of shear effects is essential for safe and realistic evaluation of strength and ductility of reinforced concrete frames because shear-critical frames continue to be found in practice.

2. Most available tools either ignore shear effects altogether, employ rudimentary shear models, or are overly-complex, requiring precalculation of shear hinge properties using separate software and selection of numerous analysis options. Typically, they result in severe overestimations of strength and ductility in shear-critical structures.

3. Classical stiffness-based frame analysis algorithms provide a simple, fast, and accurate analytical base for the implementation of nonlinear sectional fiber models.

4. The implementation of an unbalanced force approach, combining linear-elastic frame analysis algorithms with nonlinear sectional analysis routines, provides a suitable platform for accurate modeling of the nonlinear behavior of frame structures.

5. The implementation of the DSFM into a sectional analysis procedure produces simple and accurate simulations of the nonlinear sectional behavior of frame elements, particularly those that are shear-critical.

6. The analytical procedure developed accurately simulates the experimental responses of frame structures subjected to pushover and monotonic loads with high levels of accuracy. Strengths, stiffnesses, ductilities, and failure modes are captured accurately. Computed parameters such as crack widths, reinforcement strains, and member deformations are also simulated well.

7. Based on a total-load secant-stiffness formulation, the analytical procedure developed exhibits excellent convergence and numerical stability characteristics, requiring little computational time.

8. Further work is required to accurately model the behavior of frames heavily influenced by joint panel distress, bond slip, or compression bar buckling.

REFERENCES

Angelakos, D.; Bentz, E. C.; and Collins, M. P., 2001, "Effect of Concrete Strength and Minimum Stirrups on Shear Strength of Large Members," *ACI Structural Journal*, V. 98, No. 3, May-June, pp. 290-300.

Carr, A. J., 2005, "User Manual for the 2-Dimensional Version Ruaumoko2D," University of Canterbury, Department of Civil Engineering, Computer Program Library, 87 pp.

Collins, M. P., and Mitchell, D., 1991, *Prestressed Concrete Structures*, Response Publications, Canada, 766 pp.

CSA A23.3, 2004, "Design of Concrete Structures," Canadian Standards Association, Mississauga, ON, Canada, 214 pp.

CSI, 2005, "Analysis Reference Manual for SAP2000®, ETABS® and SAFE™," Computers and Structures, Inc., Berkeley, CA, 415 pp.

Duong, K. V.; Sheikh, S.; and Vecchio, F. J., 2007, "Seismic Behavior of Shear-Critical Reinforced Concrete Frame: Experimental Investigation," *ACI Structural Journal*, V. 104, No. 3, May-June, pp. 304-313.

Guner, S., 2008, "Performance Assessment of Shear-Critical Reinforced Concrete Plane Frames," PhD thesis, Department of Civil Engineering, University of Toronto, Toronto, ON, Canada, 429 pp. (http://www.civ.utoronto.ca/vector/) (accessed Oct. 10, 2009)

Guner, S., and Vecchio, F. J., 2008, "User's Manual of VecTor5." (http://www.civ.utoronto.ca/vector/) (accessed Oct. 10, 2009)

Guner, S., and Vecchio, F. J., 2010, "Pushover Analysis of Shear-Critical Frames: Formulation," *ACI Structural Journal*, V. 107, No. 1, Jan.-Feb., pp. 63-71.

Lefas, I. D.; Kotsovos, M. D.; and Ambraseys, N. N., 1990, "Behaviour of Reinforced Concrete Structural Walls: Strength, Deformation Characteristics, and Failure Mechanism," *ACI Structural Journal*, V. 87, No. 1, Jan.-Feb., pp. 23-31.

Sagbas, G., 2007, "Nonlinear Finite Element Analysis of Beam-Column Subassemblies," MASc thesis, Department of Civil Engineering, University of Toronto, Toronto, ON, Canada, 181 pp.

Vecchio, F. J., 1987, "Nonlinear Analysis of Reinforced Concrete Frames Subjected to Thermal and Mechanical Loads," *ACI Structural Journal*, V. 84, No. 6, Nov.-Dec., pp. 492-501.

Vecchio, F. J., 2000, "Disturbed Stress Field Model for Reinforced Concrete: Formulation," *Journal of Structural Engineering*, ASCE, V. 126, No. 9, Sept., pp. 1070-1077.

Vecchio, F. J., and Balopoulou, S., 1990, "On the Nonlinear Behaviour of Reinforced Concrete Frames," *Canadian Journal of Civil Engineering*, V. 17, No. 5, pp. 698-704.

Vecchio, F. J., and Collins, M. P., 1988, "Predicting the Response of Reinforced Concrete Beams Subjected to Shear Using Modified Compression Field Theory," *ACI Structural Journal*, V. 85, No. 3, May-June, pp. 258-268.

Vecchio, F. J., and Emara, M. B., 1992, "Shear Deformations in Reinforced Concrete Frames," *ACI Structural Journal*, V. 89, No. 1, Jan.-Feb., pp. 46-56.

Vecchio, F. J., and Shim, W., 2004, "Experimental and Analytical Reexamination of Classic Concrete Beam Tests," *Journal of Structural Engineering*, ASCE, V. 130, No. 3, pp. 460-469.